J Electr Eng Technol.2018; 13(5): 1901-1907
http://doi.org/10.5370/JEET.2018.13.5.1901

ISSN(Print) 1975-0102
ISSN(Online) 2093-7423

# Practical Calculation of Iron Loss for Cylindrical Linear Machine

**Sung-In Jeong**†

**Abstract** – This paper is a study for accurate iron loss calculation of a cylindrical linear machine for free piston engine. This study presents that it is possible to accurately predict power loss in ferromagnetic laminations under magnetic flux by specially considering the dependence of hysteresis, classical, and excess loss components on the magnetic induction derivative. Significant iron loss in the armature core will not only compromise the machine efficiency, but may also result in excessive heating, which could lead to irreversible deterioration in the machine performance. Thus, correct prediction of power losses under a distorted flux waveform is therefore an important prerequisite to machine design, particularly when dealing with large apparatus where stringent efficiency standards are required. Finally, it will be discussed about the iron loss in various materials of cylindrical linear electric machine by geometric and electrical parameters. It will give elaborate information about the perfect design and design rules of cylindrical linear machine and in parallel tools for the calculation, simulation and design will be available.

**Keywords**: Cylindrical linear machines, Eddy current loss, Excess loss, Ferromagnetic, Free piston engine, Hysteresis loss, Soft magnetic composite.

## 1. Introduction

Among the various linear electric machines, cylindrical types with magnet excitation are particularly popular, since they hardly experience typical assembly problems of linear machines ; conforming to a compact structure and a low weight compared with the force. As a result, recently cylindrical linear permanent magnet machine became an attractive candidate for servo systems in need of high precision control and for free piston engine. Especially, it is important to increasing efficiency by reduction of losses in application fields such as free piston engine [1]. The losses depend on the kinds of the materials and operating frequencies of cylindrical linear machine. The cylindrical type linear machines include an armature and a translator. The former consists of a single conductive wire cylindrically wound and encapsulated, while the latter is a cylindrical assembly of sintered NdFeB permanent magnets arrayed at an axial North-South stack contained in an encasing tube. The physical configuration is shown in Fig. 1.

A permanent magnet generator of cylindrical linear type with back-iron in the mover can be used especially in hybrid vehicles to power traction drives due to its high force density, wide speed range, and high efficiency. In particular, the back-iron core in this mover structure has a double face ; one is the advantage that its establishment causes an efficient flux path, the other is that it leads to the increasing of the material cost due to adding of the iron core volume.

† Corresponding Author: Dept. of IT-Automotive Engineering, Gwangju University, Korea. (si.jeong@gwangju.ac.kr)
Received: November 28, 2017; Accepted: March 30, 2018

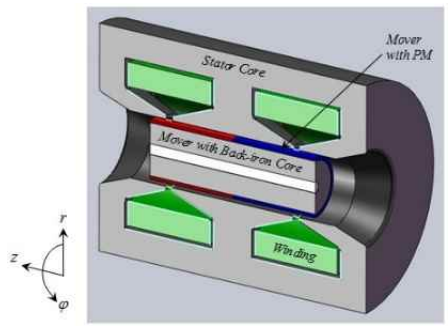


**Fig. 1.** Cylindrical Linear Machine

Therefore, this study will investigate the various losses for the sake of the accurate performance evaluation of the machine ; copper loss, eddy-current loss of the permanent magnet and iron loss consisting of hysteresis, eddy current, and excess loss.

## 2. Calculation of Iron Loss

First of all, the calculation of the iron loss with the help of the *Steinmetz* equation is still used at high frequencies up to 1000 [Hz] in the field of automotive applications, but it is no longer accurate enough. Thus, the theory of *Bertotti* is recommended as a newer approach, in which the iron losses are composed of the three components : hysteresis, eddy-current and excess loss. Here, the excess loss describes that the loss incurred in the magnetizable domains of the material with the migration of block wall and it is still based on empirical factors from curve fitting [2].

The total iron loss $P_{iron}$, i.e., the loss which is absorbed by a unit mass, is commonly separated into three contributions.

$$P_{iron} = P_{hyst} + P_{ed} + P_{excess} \quad (1)$$

The individual parameter of the loss equations must be adjusted to measured data by Epstein or Single Sheet Tester. There are proposals to describe these losses with empirical equations with up to 8 parameters in relation to the iron loss. In order to build more favorable and accurate assessment, the total iron loss will be achieved based on a physical approach using the material data and the sheet thickness [3]. The material information can be obtained by the manual of relevant manufacturer.

## 2-1 Hysteresis loss

The specific hysteresis loss can be described by the following equation according to [3].

$$P_{hyst} = k\frac{4H_c}{\rho}B_{\max}\cdot f \quad (2)$$

The hysteresis loss $P_{hyst}$ corresponds to the area of the static hysteresis loop multiplied by frequency $f$. For a rectangular shaped hysteresis loop with the coercivity $H_c$ and maximum induction level $B_{max}$ an approximation can be given by Eq. (2). The $\rho$ is the material density and $k$ is a dimensionless constant, which is close to 1 for a rectangular shape hysteresis loop

Compared with the measurement in *Epstein*, the hysteresis loss deteriorates considerably through the manufacturing process. The main factors here are caused by not only the structural changes at the plate contour from the stamping process or laser cutting, but also mechanical stresses in the packaging or the mounting of the stator core.

By a magnetic annealing after punching, the punching-related micro structural changes can be eliminated. Also, an insulating oxide layer or a phosphating is applied to the metal sheet by annealing process (*Ludwig* process). In this case, the advantage is also the extensive removal of burrs that affect the eddy-current loss unfavorable. The hysteresis loss is increased by the additional processing allowance $k_{bh}$ considering the influences of the manufacturing technology. For stamped and not finally annealed metal sheets usually $k_{bh}$=1.5 is used.

## 2-2 Eddy current loss

The eddy-current loss which arises by the swirling in the sheet edges is predictable by the conductivity $\sigma$ and thickness $d$ with a simple approach from the classical *Maxwell* Equations.

$$P_{ed} = \frac{\pi^2\sigma\cdot d^2}{6\rho}B_{\max}^2\cdot f^2 \quad (3)$$

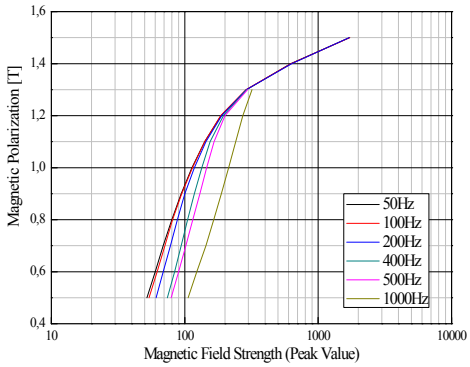


**Fig. 2.** Influence of the Frequency of the Magnetization Curve [4], (Quote : Material Specification M250-35, *Thyssen Krupp*)

In most cases, the approach does not take displacement current into account because the sheet thickness is so small that the effect is negligible. By the quadratic influence of sheet thickness and the frequency, thin sheets should be used preferably at high supply frequency. For higher frequency eddy-current losses grow to the main contribution to total loss. For a strip material of 0.1 [mm] thickness this is the case at a few kHz and for 0.35 [mm] thickness at a few hundred Hz. A retroactive effect of the eddy currents also arise at high frequency on the magnetic field, as a result it gives rise to a change of the magnetization curve. This is especially related to currents containing harmonic components as a result of converter supply, where higher frequency harmonics by ampere turns result in significantly smaller induction amplitudes, therefore it leads to smaller loss (decreasing by $B^2$). It can be shown that no difference in the eddy-current loss as a function of, e.g., the clock frequency of the inverter occurs for a frequency-independent magnetization curve.

The influence of manufacturing technology must be taken into account by an additional processing allowance $k_{bh}$ again. It results from cutting-air of punch and also by tool wear, mostly the stamping burrs. Particularly, thin sheets ($d \leq 0.1[mm]$) are critical, in which laser- or water jet cutting is preferred.

Also the burr-free sheets with laser method can be produced in proper process control when the laser cutting is still more expensive than the punching. The ridges at the punched sheet metal may be removed after the packaging by etching of the air-gap surfaces with 30 [%] phosphoric acid. However, this process step is to be integrated poorly in a series production. In a few cases, the wire cutting process is used. For this purpose, the circular blanks are only adhesively bonded to a package (baked varnish technology) and then eroded out the slot and air-gap contour. The conclusions between the individual sheets can be largely prevented through a careful process control. The pollution of the dielectric (pure water) by the burn-up of the baking lacquer layers must be removed by continuous

changes of water. Typical values for the eddy-current additional processing allowance is in punched sheets with $k_{bh}$ = 1.5~2.5.

### 2.3 Excess loss

This loss was described by *Bertotti* for the first time and can be attributed to the magnetic domain structure of the material with sliding *Bloch* walls. During magnetization the *Bloch* walls cannot be moved unresistingly, so that an additional energy demand arises. This loss strongly depends on the microscopic structure and the distribution of magnetizable domains in material, is also more statistical nature and only occurs at frequencies above 300 ~ 400 [Hz] significantly.

$$P_{exc} = \frac{C}{\rho} B_{\max}^{1.5} \cdot f^{1.5} \tag{4}$$

The factor $C$ is the second adjustable factor in measurements and in principle inversely proportional to the number of available magnetizable domains in the considered cross-section. Since the inner structure of material is fixed after the rolling process, it can be assumed that a manufacturing process influence is generally negligible. Unless that the inner crystalline structure of the material is changed dramatically, e.g., by bending or other deformations of the sheets.

### 2.4 Total losses

The three loss components can be summarized as follows Eq. (5) :

$$P_{fe} = \frac{1}{\rho}\left( 4kH_c B_{\max} f \cdot k_{bh} + \frac{\pi^2 \sigma \cdot d^2}{6} B_{\max}^2 f^2 \cdot k_{bw} + C B_{\max}^{1.5} f^{1.5} \right) \tag{5}$$

A fit can be easily achieved again by adjusting $k$ and $C$ with the measured values of material data sheets.

## 3. Comparison of the Iron Loss Calculation using Example M250-35

According to the material data sheet of *ThyssenKrupp*, this material has the following parameters :

**Table 1**. Material Data Sheet of M250-35 [4]

| | |
|---|---|
| Sheet Thickness, $d$ | 0.35 [$mm$] |
| Relative Permeability at 1 [T], 50 [Hz] | 7018 |
| Density, $\rho$ | 7600 [$kg/m^3$] |
| Conductivity, σ | $1.67\times10^6$ [$1/\Omega m$] |
| Coercive Force, $H_c$ | 30 [$A/m$] |

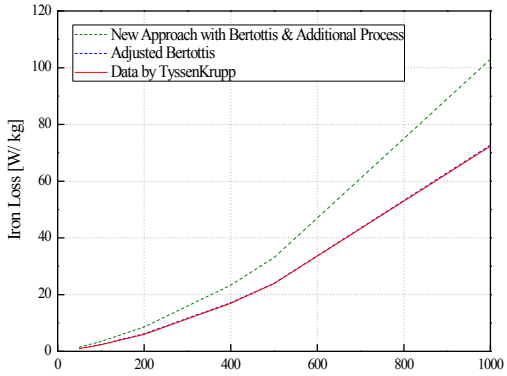


**Fig. 3.** Parameter Adjustment of the Loss Equations to the Measured Data, $k$=1, $C$=3.1. (Additionally, the influence of technology factors is entered with $k_{bh}$=$k_{bw}$=1.5)

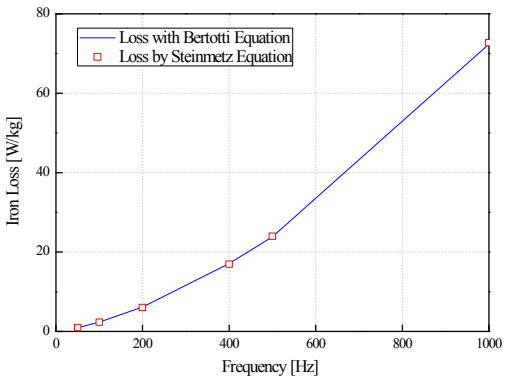


| Frequency | *Bertotti* | *Steinmetz* |
|---|---|---|
| [Hz] | [W/kg] | |
| 50 | 0.95 | 0.915 |
| 100 | 2.36 | 2.29 |
| 200 | 6.159 | 5.99 |
| 400 | 17.12 | 16.91 |
| 500 | 23.87 | 23.949 |
| 1000 | 72.36 | 72.672 |

**Fig. 4.** Comparison of Losses by *Steinmetz* and *Bertotti*

The factors $k$ and $C$ were adjusted for the frequency range 50~1000 [Hz] with $k$=1 and $C$=3.1 on the loss table for $B_{max}$ = 1 [T]. The comparison of the curve fitting with the measured losses is shown in Fig. 3.

The fit according to Eq. (4) is almost perfect, the error is negligible. Fig. 4 shows the comparison of the new equation and the *Steinmetz* equation for the frequency range up to 1000 [Hz].

It is clear that the loss by *Steinmetz* are calculated somewhat lower up to 400 [Hz], also provides the *Steinmetz* equation too pessimistic values. A description of the eddy-current loss with a purely quadratic function approach is not satisfied any more in this frequency range. Where the curves intersect, the choice of interpolation points for the *Steinmetz* equation is achieved (here 50 [Hz] and 500 [Hz]). As shown in figure 2, the new equation is much more accurate in the entire frequency range.

**Table 2.** Material Data Sheet of M400-50 [5]

| | |
|---|---|
| Sheet Thickness, $d$ | 0.5 [$mm$] |
| Relative Permeability at 1 [T], 50 [Hz] | 5927 |
| Density, $\rho$ | 7700 [$kg/m^3$] |
| Conductivity, $\sigma$ | $2\times10^6$ [$1/\Omega m$] |
| Coercive Force, $H_c$ | 50 [$A/m$] |

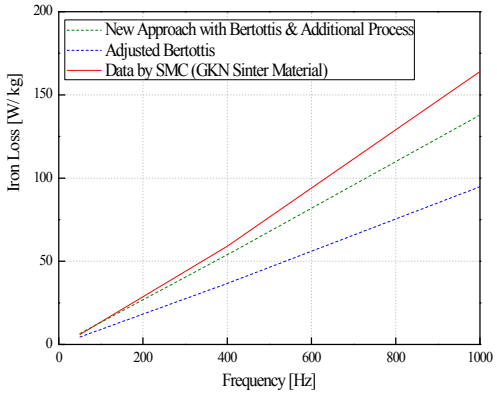


**Fig. 5.** Loss Adjustment for M400-50 Measured at the Sampling Points, $k$=1, $C$=1, $C$=1, $B_{max}$=1[T] Green Dash Line : Technology Factors with $k_{bh}$=$k_{bw}$=1.5

## 4. Iron Loss Analysis for using Example M400-50

The method presented here will be applied to other types of electrical steel.

### 4.1 Iron losses for the sheet grade M400-50

Here, a good fit is also achieved to the loss data of the material data sheet. The other sheet data is reported according to Table 2.

Fig. 5 shows the loss at $B_{max}$=1[T] with the parameters $k$=1, $C$=1.

The maximum error occurs approximately 38 [%] at 1000 [Hz]. The error results in somewhat higher loss than measured value. It is negligible in most of the applications if the technology factors $k_{bh}$ and $k_{bw}$ is mathematically taken into account. The reason should be sought in the eddy-current term, since skin effect is already expected at these thicknesses below 1000 [Hz].

### 4.2 Calculation of iron loss improvement of the approach for eddy current loss

The Eq. (5) based on *Bertotti* Theory can be trusted with respect to the eddy-current loss of a linear current density distribution over the cross section of sheet metal. This approach is largely justified with relatively thin iron-silicon sheets up to 0.5 [mm] and frequencies up to 500 [Hz]. At higher conductivity of the material and higher frequencies, this eddy-current term is too inaccurate. Then the skin effect, i.e., non-linear current density distribution can be taken into account over the cross-section of the sheet.

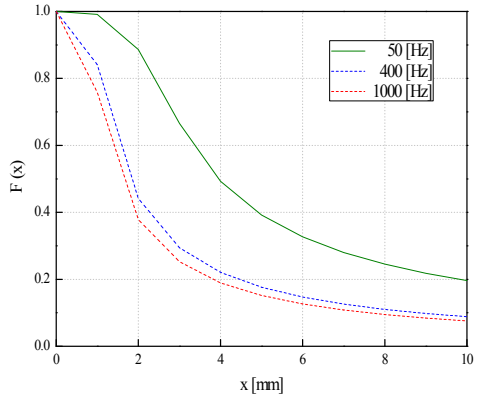


**Fig. 6.** The Calculation of the Eddy Current Loss, M400-50A

The eddy-current loss that occurred in the plate edges by the eddy current is no longer simple relationship as shown in the Eq. (3) [3].

$$F(x) = \frac{3}{x}\cdot\frac{\sin h(x)-\sin(x)}{\cos h(x)-\cos(x)} \tag{6}$$

$$x=\beta\cdot d \tag{7}$$

$$\beta = \sqrt{\pi\cdot f\cdot\sigma\cdot\mu} \tag{8}$$

With retroactive effect of the current on the exciting field, the calculation is performed ; for example, it is analogous to the calculation of the unilateral skin effect under solution of the *Maxwell* Equations for the magnetomotive force, the induction and *Ohm's* Law. This is described in detail in [6]. The function occurring here is shown in figure 6.

The effective value of the current density results in

$$|J| = J = \beta\cdot\sqrt{2}\,H_0\,\frac{\sqrt{\cos h\,2\beta\cdot y-\cos 2\beta\cdot y}}{\sqrt{\cos h\,\beta\cdot d+\cos\beta\cdot d}} \tag{9}$$

where, $y$ represents the coordinate iron sheet thickness.

It should be noted that the permeability depends on the flux density and is also frequency-dependent. In most case, this is listed on the material data sheets. The frequency dependence of the induction distribution and the current density distribution over the plate thickness is shown on the example of the material M400-50 in figure 6 and figure 7 on a flux density amplitude of 1 [T]. It can be seen that as the frequency increases, the distribution of $B$ is always uneven while the amplitude of the eddy-current density $J$ increases toward the edge, but it still remains largely linear over the sheet thickness in the frequency range. Generally, it is used from 0.1 to 0.2 [mm] of the iron sheet thickness over 1000 [Hz] of frequency. Further obtained from [6] for the eddy-current loss in the volume $V$ of the sheet.

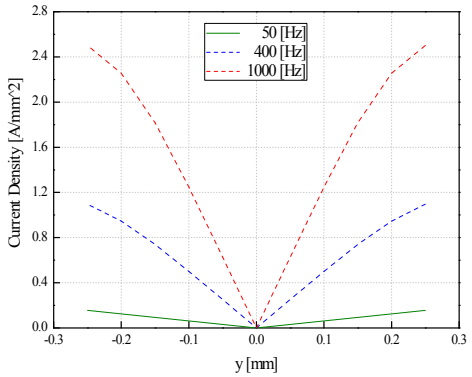


**Fig. 7.** Current density J (y) by the plate thickness, M400-50A

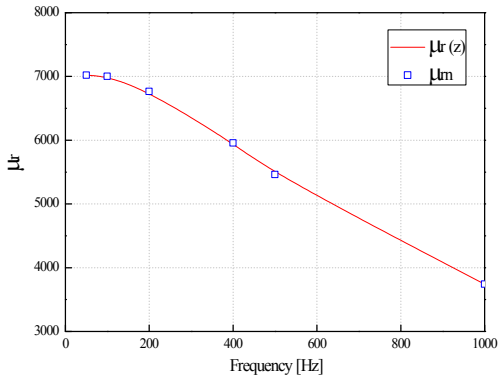


**Fig. 8.** Adaptation of the logarithmic approximation $\mu_r(Z)$, Measured Values for $\mu_{rn}(f2n)$ (M250-35A, $B_{max}$=1 [T], 50 [Hz] ≤ f ≤ 1000 [Hz])

$$P_{ed} = V\frac{1}{\sigma \cdot d}\int_{-\frac{d}{2}}^{+\frac{d}{2}} J^2\, dy = V\frac{1}{6}\sigma\pi^2 f^2 d^2 B_{\max}^2 \frac{3}{x}\cdot\frac{\sin h(x)-\sin(x)}{\cos h(x)-\cos(x)} \tag{10}$$

That is, the loss of Eq. (3) is supplemented by the additional term with the hyperbolic and the $x$, which corresponds to the unilateral skin effect of the reduced conductor height. Since the fraction term in Eq. (10) goes to $3/x$ at high frequencies, the loss increases proportionally at constant flux density to $d \cdot f^{1.5}$ and no longer square. Division of Eq. (10) by the mass $M=V \cdot \rho$ provides the specific eddy-current loss.

$$P_{ed} = \frac{\pi^2 \sigma \cdot d^2}{6\rho} B_{\max}^2 f^2 \frac{3}{x}\frac{\sin h(x)-\sin(x)}{\cos h(x)-\cos(x)} \tag{11}$$

The necessary permeability for the evaluation of this equation must be taken from the material sheet in accordance with the flux density $B_{max}$ and the frequency. Namely if this extended equation is to be used, the design calculation of the magnetization curve must be known for determination of $\mu_r$ for the respective frequency. This can be done by interpolation of the given $\mu_r$ values. For a given induction, a plot $\mu_r(f)$ through logarithmic function of the type

$$\mu_r(f) = a \cdot \ln(f) - b \cdot f^{\frac{1}{2}} + c \tag{12}$$

with the constants $a$, $b$, $c$ good approach (figure 8), which facilitates the analytical calculation a little.

Then, the total loss of Eq. (5) result in

$$P_{fe} = \frac{1}{\rho}\left( 4\,k\,H_c\,B_{\max}\,f \cdot k_{bh} + \frac{\pi^2 \sigma \cdot d^2}{6} B_{\max}^2 f^2 \cdot \frac{3}{x}\frac{\sin h(x)-\sin(x)}{\cos h(x)-\cos(x)} k_{bw} + C\,B_{\max}^{1.5} f^{1.5} \right) \tag{10}$$

A fit can easily achieve again by adjusting $k$ and $C$ with the measured values of material data shee ts. Carrying the frequency-dependent permeability, however, makes sense only if corresponding data is available or can be measured.

**Table 3.** Material Data Sheet of PM4EM11 in GKN Sinter Metals [7]

| | |
|---|---|
| Sheet Thickness, $d$ | 0.5 [$mm$] |
| Density, $\rho$ | 7500 [$kg/m^3$] |
| Static rel. Permeability at 1 [T] | 472 |
| Conductivity, $\sigma$ | $3.571\times10^{-9}$ [$1/\Omega m$] |
| Coercive Force, $H_c$ | 249 [$A/m$] |

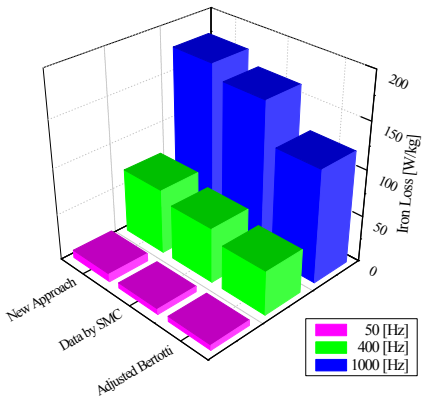


| | $B_{max}$= 1 [T] | | |
|---|---|---|---|
| Frequency [Hz] | 50 | 400 | 1000 |
| Data by SMC (PM4EM11 GKN Sinter Metals) | 6.0 | 59.0 | 164.0 |
| Adjusted *Bertottis* | 5.74 | 47.29 | 121.31 |
| New Approach with *Bertottis* & Additional Process | 8.56 | 69.86 | 177.75 |

**Fig. 9.** Parameter Fit for GKN Sinter Metals, $k=0.85$, $C=2$, $k_{bh}=k_{bw}=1.5$, Max. Error in 50 [Hz] = 0.67 [%], 400 [Hz] = 1.48 [%], and 1000 [Hz] = 1.46 [%]

## 5. Comparison of the Iron Loss using Example Soft Magnetic Composites

The adjustment to the support points of the measured loss values on the material sheet [7] made for 0.5 [mm] sheet thickness. For SMC frequency-dependent permeability values are not available for the time. Therefore it could be used here only the static permeability, whereby the curve fitting has a provisional nature.

The absence of frequency-dependent permeability are obtained for $k$ and $C$ in both cases physically unrealistic values, although the fitting must be regarded as good and easier to perform than without taking into account the current displacement.

## 6. Comparison Result

In conclusion, the research of the iron losses of the stator and mover is carried out by analytical and numerical calculation. The actual values of each loss make it possible to predict the machine performance and allow us to make a design of process occurring in the machine.

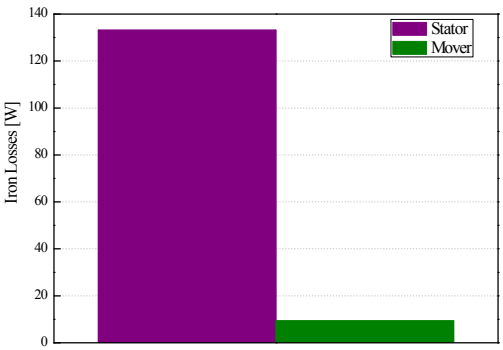


| Loss | [W] |
|---|---|
| Stator | 133.15 |
| Mover | 9.39 |

**Fig. 10.** Comparison of Losses, $k$=1, $C$=1, $k_{bh}$=$k_{bw}$=1.5, in 50 [Hz]

Among the whole losses of the machine, the iron loss consisted of the stator and mover part is the best part of the losses which is approximately 70[%]. The ratio of the stator and mover in iron loss is only 9.3 to 0.6 ; i.e., the iron loss in stator is significantly greater than that in mover due to larger volume. Figure 10 indicates the information of losses in each armature core region.

## 7. Conclusion

Different analytical approaches are developed and proposed for calculating both the stator field and slotting based losses. Many application areas demand analytical results for realistic model incorporating the appropriate nonlinear effects. For instance, practical design considerations require that some degree of saturation occurs in the magnetic circuit of the electrical generator. First, it deals with the nonlinearity of saturation overlooked in the previous study using equivalent magnetic circuit. Based on this analytical calculation, the numerical calculation is carried out using FLUX 2-D of FEA software. And then, it is compared and evaluated with the results between analytical and numerical calculation. As a result, it shows that the results are in agreement with each other. Moreover, the weight of generator is investigated by kinds of the material and region in terms of the material cost and thermal analysis beforehand. This approach is extended to accurate prediction of power loss for detailed design. It is classified by two kinds of iron loss ; stator and mover iron loss. Here, the iron loss is analyzed through different types of material, and is also considered by three components of losses ; hysteresis, classical, and excess loss.

Finally, it will make the analysis of the machine perfect by considering the nonlinearity and losses of the materials selected for cylindrical linear machine. Moreover, this analysis results is also achieved in thermal distribution characteristics continuously.

## Acknowledgements

This study was conducted by research funds from Gwangju University in 2018.

## Reference

[1] Sung In Jeong, *Comparative Study of Linear Oscillating Generators*, Dissertation an der Technischen Universität Braunschweig, 2015

[2] Prof. Dr.-Ing. W.-R. Canders, "Berechnung von Eisenverlusten Physikalisch basierter Ansatz nach Bertottis Theorie," *TB 13-03-03*

[3] W. Pieper and J. Gerster, "Total power loss density in a soft magnetic 49% Co-49% Fe-2% V-alloy," *Journal of Applied Physics 109*, 07A312 (2011)

[4] Material Specification, *ThyssenKrupp, M250-35*

[5] Material Specification, *ThyssenKrupp, M400-50*

[6] Küpfmüller, *Einführung in die Theoretische Elektrotechnik*, Springer Verlag, Berlin, Heidelberg, New York, 1968

[7] http://www.gkn.com/sintermetals/capabilities/soft-magnetic-pm/Pages/materials.aspx

**Sung-In Jeong** He received B.S. and M.S. degrees in Electrical Engineering from Dongguk and Hanyang University, South Korea, respectively. And then he was responsible for the development of electrical machine and its drive at Samsung Heavy Industry, Samsung Electronics, and Daewoo Electronics, in order. After he received Dr.-Ing. degree from Technical University Braunschweig, Germany. He was in the Daelim Motor, South Korea. Since March 2018, he has joined Gwangju University, where he is currently a Professor in the Division of IT-Automotive Engineering. His research and development field and interest included design, analysis and drive of electric machine for electric and smart personal motilities.